NASA TECHNICAL MEMORANDUM

NASA TM X-3373

NASA TM X-3373

EFFECT OF FLAME STABILIZER DESIGN ON PERFORMANCE AND EXHAUST POLLUTANTS OF A TWO-ROW 72-MODULE SWIRL-CAN COMBUSTOR

James A. Biaglow and Arthur M. Trout

Lewis Research Center

Cleveland, Ohio 44135

NATIONAL AERONAUTICS AND SPACE ADMINISTRATION • WASHINGTON, D. C. • MARCH 1976

1. Report No.	2. Government Accession No.	3. Recipient's Catalog No.
NASA TM X-3373		

4. Title and Subtitle EFFECT OF FLAME STABILIZER DESIGN ON PERFORMANCE AND EXHAUST POLLUTANTS OF A TWO-ROW 72-MODULE SWIRL-CAN COMBUSTOR	5. Report Date March 1976
	6. Performing Organization Code
7. Author(s) James A. Biaglow and Arthur M. Trout	8. Performing Organization Report No. E-8564
	10. Work Unit No. 505-03
9. Performing Organization Name and Address Lewis Research Center National Aeronautics and Space Administration Cleveland, Ohio 44135	11. Contract or Grant No.
	13. Type of Report and Period Covered Technical Memorandum
12. Sponsoring Agency Name and Address National Aeronautics and Space Administration Washington, D. C. 20546	14. Sponsoring Agency Code

15. Supplementary Notes

16. Abstract

A test program was conducted to evaluate the effects of four flame stabilizer designs on the performance and gaseous pollutant levels of an experimental full-annular swirl-can combustor. Combustor operating parameters, including inlet-air temperature, reference velocity, and fuel-air ratio, were set to simulate conditions in a 30:1 pressure ratio engine. Combustor inlet total pressure was held constant to 62 N/cm^2 (6 atm) due to the facility limit. Combustor performance and gaseous pollutant levels were strongly affected by the geometry and resulting total pressure loss of the four flame stabilizer designs investigated. The addition of shrouds to two designs produced an 18 to 22 percent decrease in the combustion chamber pressure loss and thus resulted in doubling the exit temperature pattern factor and up to 42 percent higher levels of oxides of nitrogen. A previously developed oxides of nitrogen correlating parameter agreed with each model within an emission index of ±1 but was not capable of correlating all models together.

17. Key Words (Suggested by Author(s))	18. Distribution Statement
Turbojet engines; Gas turbine engines; Combustion chambers; Exhaust gases; Combustion products; Air pollution; Hydrocarbon combustion; Carbon monoxide; Nitrogen oxides	Unclassified - unlimited STAR Category 07

19. Security Classif. (of this report)	20. Security Classif. (of this page)	21. No. of Pages	22. Price*
Unclassified	Unclassified	22	$3.25

* For sale by the National Technical Information Service, Springfield, Virginia 22161

EFFECT OF FLAME STABILIZER DESIGN ON PERFORMANCE AND EXHAUST POLLUTANTS OF A TWO-ROW 72-MODULE SWIRL-CAN COMBUSTOR

by James A. Biaglow and Arthur M. Trout

Lewis Research Center

SUMMARY

A test program evaluated the effects of four flame stabilizer designs on the performance and gaseous pollutant levels of an experimental full-annular 72-module swirl-can combustor. Combustor operating parameters, including inlet-air temperature, reference velocity, and fuel-air ratio, were set to simulate conditions in a 30:1 pressure ratio turbofan engine. Combustor inlet total pressure was held constant at 62 newtons per square centimeter (6 atm) due to the facility limit. Combustor performance and gaseous pollutant levels were strongly affected by the geometry and resulting total pressure loss of the four flame stabilizer designs investigated. The addition of shrouds to two designs produced an 18 to 22 percent decrease in the combustion chamber pressure loss and thus resulted in doubling the exit temperature pattern factor and up to 42 percent higher levels of oxides of nitrogen. A previously developed oxides of nitrogen correlating parameter agreed with each model within an emission index of ±1 but was not capable of correlating all models together.

At simulated subsonic cruise test conditions the use of a flame stabilizer design incorporating contraswirl produced the lowest oxides of nitrogen emission index level of 9.1 grams per kilogram of fuel at an average exit temperature of 1468 K. At simulated takeoff, the use of a solid circular flame stabilizer produced the lowest oxides of nitrogen emission index level of 15.1 grams per kilogram of fuel at an average exit temperature of 1495 K.

INTRODUCTION

Four flame stabilizer designs were investigated in a full-annular 72-module swirl-can combustor to determine their effects on combustor performance and exhaust gas pollutants. The tested designs included contraswirl for increased mixing in the wake of swirl-can modules and shrouds that delayed introduction and mixing of the bypass air into the module wake.

The performance and exhaust pollutants of aircraft engines are of major concern in the vicinity of airports and in the stratosphere. The 1979 EPA standards require aircraft engines to be greater than 99.0 percent efficient during idle and taxi and to reduce oxides of nitrogen by 75 percent over conventional aircraft. Previous studies of swirl-can combustors (refs. 1 and 2) have shown the capability of approaching these goals with greater than 98.0 percent efficiency at idle and a reduction of 50 percent in oxides of nitrogen at takeoff.

Recent single module and seven module swirl-can tests (refs. 3 and 4) have shown the potential for even further reductions in the level of oxides of nitrogen. These module tests included various flame stabilizer designs of minimum recirculation zone size with high recirculation zone strength for reduced NO_x formation. However, added data were needed to determine how effective they would be in a full-scale annular swirl-can combustor. In an effort to apply the single module and seven module results to a full annular combustor, four flame stabilizer designs were investigated. The test designs included a solid circular flame stabilizer with and without shrouds and contraswirl flame stabilizers with and without shrouds. The solid circular flame stabilizer would provide a base model for comparing the individual effects of shrouds and contraswirl and also the combined effect of contraswirl with shrouds. Testing the different designs would also add valuable information for developing an oxides of nitrogen correlating parameter.

Tests were conducted using a two-row 72-module swirl-can combustor operating at simulated subsonic cruise and takeoff conditions typical of a 30:1 pressure ratio turbofan engine. Combustor operating parameters except inlet pressure were the same as in an engine. Operating conditions were as follows: Inlet air temperature, 733 to 858 K; inlet total pressure, 62.0 newtons per square centimeter; combustor reference velocity, 30.5 to 36.6 meters per second; average exit temperature, 1477 K. All tests were performed with ASTM Jet A fuel.

APPARATUS

Combustor Design

The combustor used in this program was the swirl-can combustor whose performance was evaluated at idle conditions in reference 1. A cross-sectional sketch of this combustor is shown in figure 1. The combustor was installed in an annular housing that had an outer diameter of 1.062 meters, an inner diameter of 0.54 meter, and was 0.514 meter long. The inlet diffuser passage of the combustor was 12.95 centimeters long and had an exit to inlet area ratio of 1.2. The diffuser was followed by a sudden expansion region in which the ratio of the annular flow area at the inlet plane of the swirl cans

divided by the diffuser exit area was 2.85. The swirl-can modules were mounted to the liners and attached to each other by means of gussets as shown in figure 2. The fuel tubes entered from the upstream side and were centered in the swirl cans by means of tabs located on the ends of the fuel tubes.

Combustor Configurations

Four combustor flame stabilizer configurations were investigated:

(1) Model I - circular flame stabilizer design of reference 1 and shown in figure 3

(2) Model S-I with a 1.27 cm long shroud around the perimeter of the circular flame stabilizer in figure 4

(3) Model II - a circular flame stabilizer designed to produce a contraswirl around each swirl can in figure 5

(4) Model S-II with a shroud around the contraswirl flame stabilizer in figure 6

The module designs investigated in this report were similar to those in references 3 and 4 except that the solid flame stabilizers were circular and the contraswirl was produced by radial tabs rather than vanes. In addition, the shrouds were added to the downstream edge of the flame stabilizer rather than surrounding the outer perimeter of the flame stabilizer and extending equally upstream and downstream. The outer diameter of the four flame stabilizers investigated was 5.71 centimeters. The open area of the contraswirl flame stabilizer was 2.48 square centimeters. The perforated plate seen in all four of the previous flame stabilizer figures was added to prevent excessive airflow to the hub and tip regions of the test combustor. The holes in the circular flame stabilizers of figure 4 were added to provide localized cooling to the shrouds to maintain adequate clearance for air flow between the shrouds and the liners. The physical blockage of the combustor was a nominal 67.8 percent for the solid flame stabilizer designs and 62.0 percent for the contraswirl flame stabilizer designs. In calculating the combustor blockage, the discharge coefficient for the swirlers and contraswirlers was assumed to be 1.0.

Test Facility

The annular swirl-can combustors were evaluated in a connected duct test facility. A diagram of the facility and a sketch of the installation is shown in reference 5. Airflow rates and combustor pressures were regulated by remotely controlled valves upstream and downstream of the test section. A more complete description of the test facility is included in reference 6.

Instrumentation

Combustor-inlet pressures and temperatures were measured at the locations shown in figure 7. Combustor-exit total pressures and temperatures were measured in 3° circumferential increments by three equally spaced, traversing, five-point probes. Airflow rates were measured with an air orifice installed in accordance with ASME specifications. Fuel flow rates were measured with turbine flowmeters. Descriptions of the traversing combustor-exit probe and the data acquisition and recording system are contained in references 6 and 7.

Combustor exhaust gas samples were obtained by means of three five-point traversing probes equally spaced between the combustor-exit temperature and pressure probes. The exhaust gas samples from the three probes were collected into a common line that was maintained at a minimum temperature of 422 K. The sample line was connected to four gas analyzing instruments (fig. 8). The instruments were capable of measuring concentrations of unburned hydrocarbons, carbon monoxide, carbon dioxide, and oxides of nitrogen. Figure 9 is a schematic diagram of the gas sampling system. The hydrocarbon content of the gas sample was measured by a Beckman model 402 hydrocarbon analyzer. The carbon monoxide and carbon dioxide concentrations were determined by two Beckman model 315B nondispersive infrared analyzers. Oxides of nitrogen (NO_x) were measured by a Thermo-Electron Model 10A Chemiluminescent analyzer. This instrument provided separate measurements of nitric oxide (NO) and oxides of nitrogen (in the form of $NO + NO_2$).

PROCEDURE

Test Conditions

Tests were conducted over a range of fuel-air ratios at combustor operating conditions simulating subsonic cruise and takeoff for a high pressure ratio (30:1) turbofan engine. All combustor operating parameters except inlet total pressure, which was facility limited, were as in an actual engine. Nominal combustor operating conditions for subsonic cruise, takeoff, and intermediate test conditions are listed in table I.

Combustion efficiency. - Combustion efficiency was determined by exit thermocouple measurement and by exhaust gas analysis. The thermocouple efficiency was determined by dividing the measured temperature rise across the combustor by the theoretical temperature rise. Combustion efficiency by exhaust gas analysis was determined by using

$$\eta_{gs} = 100 - 0.1\ EI_{hc} - \frac{EI_{co}}{42.7}$$

where EI_{hc} and EI_{co} are the emission index values for unburned hydrocarbons and carbon monoxide, respectively.

Reference velocity. - Reference conditions were based on the total airflow, the inlet-air density using the total temperatures and pressure at the diffuser inlet, and the reference area (3992 cm^2). The reference area was determined by the maximum cross-sectional area between the liners.

Exit temperature pattern factor $\bar{\delta}$. - The radial profile of exit temperature, which was established from the circumferential average of the temperature at each radial position, was plotted as a deviation from the average exit temperature as a function of radial position. To detect temperature nonuniformities which may not be evident in the average radial profile, the exit temperature pattern factor was calculated to reflect the magnitude of nonuniformity caused by maximum local temperatures. This factor was defined as

$$\bar{\delta} = \frac{T_{max} - T_{av}}{T_{av} - T_{in}}$$

where T_{max} is the maximum individual exit temperature, T_{av} the mass-weighted average exit temperature, and $T_{av} - T_{in}$ the temperature difference between the mass-weighted average exit temperature and the average inlet temperature. Low pattern factors in the 0.20 range indicate good exit-temperature distribution and uniformity with no undesirable hot spots.

Exhaust gas concentrations. - The concentration of measured exhaust gases (in ppm) was converted to a wet basis, as proposed in reference 8, and recorded in terms of an emission index (EI) parameter. The emission index is determined from

$$EI_x = \frac{m_x(1 + f)}{m_e f}(x)10^{-3}$$

where EI_x is the emission index in grams of x per kilogram of fuel burned, m_x the molecular weight of x, m_e the average molecular weight of exhaust gases, f the metered fuel-air ratio, and (x) the measured concentration of pollutant x in ppm.

Sample validity. - Measured values of carbon monoxide, carbon dioxide, and unburned hydrocarbons were used to determine a gas sample fuel-air ratio $(f/a)_{gs}$. These values were compared with fuel-air ratios determined by measured rates of fuel and air. Agreement between the two fuel-air ratios would indicate how well the gas sampling

probes were obtaining a representative sample of exhaust products. A gas sample validity of ±5 percent between the two fuel-air ratios was considered to be a good representation of the exhaust products.

RESULTS AND DISCUSSION

The performance and pollutant emissions for the four swirl-can test combustors were measured at simulated takeoff and subsonic cruise conditions typical of a 30:1 pressure ratio engine. The test results for the four swirl-can combustor designs are presented in the following section.

Combustor Performance

The combustor performance, including total combustion efficiency by exit-thermocouple measurement and gas analysis, pressure loss, average exit temperature, and combustor exit temperature pattern factor are presented in tables II and III. Combustion efficiency by both exit thermocouple measurement and gas analysis for the test combustors was nominally 100 percent over the entire range of test conditions. Results of the other performance parameters showed a wide variance. Test combustors having circular and contraswirl flame stabilizers (models I and II) performed with substantially better exit temperature pattern factors and emissions than the same combustor designs with shrouds (models S-I and S-II).

Variations in combustor total pressure loss with flame stabilizer design led to widespread differences in exit temperature performance of the test combustors. The combustor blockage of the unshrouded flame stabilizer configurations was 67.8 percent for the solid circular design and 62.0 percent for the contraswirl design. A nominal 10-percent reduction in pressure loss was expected due only to an increase in the open area of the flame stabilizer design by the use of the contraswirl vanes. The addition of shrouds to these two designs did not change the physical blockage of the test combustors. However, from the plot of isothermal pressure loss against inlet Mach number in figure 10, the shrouded designs produced an additional 18 to 22 percent reduction in pressure loss at an inlet Mach number of 0.22. The change in pressure loss was created by the shrouds and is discussed in details in a later section dealing with their effects.

The exit temperature pattern factor $\bar{\delta}$, which is a measure of the uniformity of the exit temperature distribution, varied according to the total pressure loss of the model investigated. The models with the best pattern factor had the highest pressure loss and those with the lowest pressure loss had the poorest pattern factor. Model I had the lowest pattern factor, 0.23 to 0.32, and the highest pressure loss. Model S-II had the

highest pattern factor, 0.57 to 0.74, and the lowest pressure loss. The high pattern factors of model S-II were responsible for the lack of subsonic cruise data and the limited takeoff data obtained for this model. Table IV shows the typical effect of changes in pattern factor with pressure loss for the four models at a inlet-air temperature of 855 K, inlet Mach number of 0.22, and a fuel-air ratio of 0.0185.

Exhaust Emissions

The exhaust emissions of oxides of nitrogen (NO_X), carbon monoxide (CO), and unburned hydrocarbons were measured. A gas sample validity of ±5 percent was maintained for most of the data.

Carbon monoxide and unburned hydrocarbons. - Emission index values of carbon monoxide and unburned hydrocarbons were less than 16.0 and 0.90 gram per kilogram of fuel, respectively. They also followed, as seen from tables II and III, the previously reported trends (ref. 5) of decreasing with decreasing inlet-air temperature and increasing with reductions in reference velocity.

Oxides of nitrogen. - Data for the total oxides of nitrogen as a function of fuel-air ratio at simulated subsonic cruise and takeoff are shown in figure 11. The data followed the previously reported trends of references 5 and 9 with the oxides of nitrogen increasing as inlet-air temperature and fuel-air ratio increased. Figure 11 also shows a substantial increase in the level of oxides of nitrogen for the shrouded over the unshrouded flame stabilizer designs. At a fuel-air ratio of 0.0185 the oxides of nitrogen for the shrouded models, S-I and S-II, were 22 to 42 percent higher than the unshrouded models, I and II.

Previous studies have shown (ref. 9) that oxides of nitrogen are strongly dependent on local flame temperature and the length of residence time of the hot gases in the primary recirculation zone of a combustor. A reduction in these quantities should lead to a corresponding decrease in the formation of oxides of nitrogen. The use of shrouds was employed in an attempt to produce a well mixed primary zone followed by a region into which the bypass air, which was delayed from being introduced into the module wake by the straight section of the shroud walls, would mix to reduce the local flame temperature. However, due to the low combustor total pressure loss which occurred with their use, the shrouds did not adequately mix the bypass air with the premixed fuel-air mixture and thus resulted in locally higher flame temperatures and increased residence time that increased the oxides of nitrogen.

NO_X correlating parameter. - Previous emission trends (refs. 9 to 11) have shown that oxides of nitrogen increase exponentially as inlet-air temperature and to a lesser degree as exit average temperature increase, but the oxides decrease with increasing reference velocity. Also, oxides of nitrogen increase with increasing combustor inlet

total pressure. The oxides of nitrogen emission index data for the test combustors are plotted in figure 12 as a function of the correlating parameter

$$\text{C. P.} = \frac{P^{1/2} e^{T_{in}/288} T_{exit}}{V_{ref}}$$

where

P combustor inlet total pressure normalized to standard sea-level pressure of $10.13\ \text{N/cm}^2$

T_{in} inlet-air temperature, K

T_{exit} exit average temperature, K

V_{ref} combustor average reference velocity, m/sec

Figure 12 shows two levels of oxides of nitrogen according to whether the test combustor used shrouded or unshrouded flame stabilizer designs. Each level includes a solid circular and a contraswirl design and follows the correlating parameter within an emission index of ±1.0. These data indicate that for combustor configurations of similar geometry, mixing characteristics and residence time, oxides of nitrogen may be accurately predicted at a given set of operating conditions if they are known at another. However, the two different levels also indicate that the correlating parameter needs to be further expanded if oxides of nitrogen are to be predicated from one combustor design to another design of different mixing and residence time. The expanded correlating parameter might include such quantities as residence time, mixing intensity, and local equivalence ratio. However, no success was achieved in the present investigation in determining the exact form for including these factors.

Effect of Shrouds

The shrouds were added to the flame stabilizer designs to produce a well mixed primary zone and to delay the introduction and mixing of the bypass air into the wake of the swirl-can modules. Since the rate of formation of oxides of nitrogen in relatively slow and dependent on local flame temperature, a small well mixed recirculation zone followed by a quenching of the local flame temperature would result in a lowering of the rate of formation of oxides of nitrogen.

The shrouds changed the air flow pattern at the flame stabilizer edge significantly but did not adequately mix the bypass air into the module wake. Each time the shrouds

were added to a flame holder design the lack of mixing was sufficient to noticeably lower the combustor total pressure drop. The lack of mixing also tended to isolate the swirl cans from each other and prevented a uniform flame path around the combustor array. The net result was localized hot spots which produce higher exit temperature pattern factors, increased residence time, and higher levels of oxides of nitrogen. Tables II and III compares the effects of the shrouded and unshrouded flame stabilizers on combustion pressure loss, exit temperature pattern factor, and oxides of nitrogen.

Figure 13 illustrates the different types of mixing that occurred with the unshrouded and shrouded flame stabilizers. In general, the flow of an air stream through a passage leading to sudden expansion produces a variety of losses depending on the geometry of the blockage in the passage. For the case of blockage from a sharp-edged plate, similar to the unshrouded flame stabilizers, losses are among the highest due to vortex shedding. This shedding produces powerful eddies and turbulence that dissipate within 8 to 10 hydraulic diameters downstream (ref. 12). When the sharp-edged blockage is modified by the addition of a transition section, such as a bellmouth, ledge, or shroud in the flame stabilizer case, the entire mixing zone reaction is altered. The resistance to air flow is lessened producing a lower total pressure loss and a mixing region more characteristic of two stream shear flow in which the airflow penetrates further downstream.

SUMMARY OF RESULTS

The combustor performance and pollution emissions were obtained for four two-row 72-module swirl-can combustors concepts operating at simulated cruise and takeoff conditions typical of a 30:1 pressure ratio turbofan engine. The following results were obtained:

1. Performance and pollution results were strongly affected by the geometry and resulting pressure loss of the four flame stabilizer designs investigated. The addition of shrouds to two designs produced an 18 to 22 percent decrease in combustion chamber pressure loss resulting in a doubling of the exit temperature pattern factor and a 22 to 42 percent increase in the level of oxides of nitrogen.

2. A previously developed oxides of nitrogen correlating parameter agreed with each model within an emission index of ±1 but was not capable of correlating all models together. Additional combustor variables such as residence time, mixing intensity, and equivalence ratio may need to be determined to develop a correlating parameter to fit all models.

3. Combustion efficiency was nominally 100 percent for the four configurations investigated with model I achieving an exit temperature pattern factor of 0.23 at an inlet-air temperature of 853 K and average exit temperature of 1457 K.

4. At simulated cruise test conditions the use of a flame stabilizer design incorpo-

rating contraswirl produced the lowest oxides of nitrogen emission index level of 9.1 grams per kilogram of fuel at an average exit temperature of 1468 K. At simulated takeoff the use of a solid circular flame stabilizer produced the lowest emission index level of 15.1 grams per kilogram of fuel at an average exit temperature of 1495 K.

Lewis Research Center,
National Aeronautics and Space Administration,
Cleveland, Ohio, January 20, 1976,
505-03.

REFERENCES

1. Aeronautical Propulsion. NASA SP-381, 1975.
2. Biaglow, James A.; and Trout, Arthur M.: Idle Efficiency and Pollution Results for Two-Row Swirl-Can Combustors Having 72 Modules. NASA TM X-3208, 1975.
3. Mularz, Edward J.; Wear, Jerrold D.; and Verbulecz, Peter W.: Pollution Emissions from Single Swirl-Can Combustor Modules at Parametric Test Conditions. NASA TM X-3167, 1975.
4. Mularz, Edward J.; Wear, Jerrold D.; and Verbulecz, Peter W.: Exhaust Pollutant Emissions from Swirl-Can Combustor Module Arrays at Parametric Test Conditions. NASA TM X-3237, 1975.
5. Biaglow, James A.; and Trout, Arthur M.: Performance and Pollution Measurements of Two-Row Swirl-Can Combustor Having 72 Modules. NASA TM X-3170, 1975.
6. Adam, Paul W.; and Norris, James W.: Advance Jet Engine Combustor Test Facility. NASA TN D-6030, 1970.
7. Rusnak, J. P.; and Shadowen, J. H.: Development of an Advanced Annular Combustor. (PWA-FR-2832, Pratt & Whitney Aircraft; NAS3-9403) NASA CR-72453, 1969.
8. Procedure for the Continuous Sampling and Measurement of Gaseous Emissions from Aircraft Turbine Engines. Aerospace Recommended Practice 1256, SAE, Oct. 1, 1971.
9. Grobman, Jack; and Ingebo, Robert D.: Jet Engine Exhaust Emissions of High-Altitude Commercial Aircraft Projected to 1990. NASA TM X-3007, 1974.
10. Schultz, Donald F.: Exhaust Emissions of a Double Annular Combustor-Parametric Study. NASA TM X-3164, 1975.

11. Diehl, Larry A.; and Biaglow, James A.: Measurement of Gaseous Emissions from a Turbofan Engine at Simulated Altitude Conditions. NASA TM X-3046, 1974.

12. Idel'chek, I. E.: Handbook of Hydraulic Resistance. Coefficients of Local Resistance and of Friction. AEC-TR-6630, Atomic Energy Commission, 1960.

TABLE I. - NOMINAL COMBUSTOR

TEST CONDITIONS

[Nominal design average exit temperature, 1477 K; inlet total pressure, 62.0 N/cm^2.]

Test condition	Inlet total temperature, K	Reference velocity, m/sec
Simulated cruise	733	30.5
Intermediate cruise	733	33.6
Simulated takeoff	858	36.6
Intermediate takeoff	858	33.6
Intermediate takeoff	828	36.6

TABLE II. - COMBUSTOR PERFORMANCE DATA

Design condition	Combustor model	Total pressure, N/cm^2	Average inlet temperature, K	Airflow, W, kg/sec	Diffuser inlet Mach number, M_3	Reference velocity, V_{ref}, m/sec	Measured fuel-air ratio, $(f/a)_m$	Mass-weighted average exit temperature, K	Pattern factor, $\bar{\delta}$	Combustor pressure, $(\Delta P/P)_{100}$, percent	Combustion efficiency, η_x, percent
Cruise	I	61.65	737	38.96	0.216	33.45	0.0164	1319	0.313	6.11	102.7
		62.55	737	38.72	.212	32.79	.0190	1410	.299	5.84	103.7
		61.65	733	39.64	.220	33.88	.0208	1473	.318	6.12	104.7
		61.76	734	39.49	.218	33.73	.0213	1488	.310	5.97	104.8
		61.84	735	39.36	.217	33.61	.0214	1401	.323	5.04	104.6
		62.23	736	40.08	.221	34.05	.0233	1540	.284	6.41	103.3
		62.45	737	35.48	.199	30.11	.0183	1374	.314	4.95	101.0
		62.43	735	35.49	.199	30.04	.0208	1454	.287	5.08	102.5
		62.63	736	35.48	.193	29.97	.0240	1563	.292	4.90	102.3
	S-I	61.86	734	39.87	0.221	33.96	0.0182	1383	0.436	5.38	103.1
		62.68	738	39.50	.216	33.42	.0200	1447	.454	5.24	103.2
		62.95	736	36.79	.200	31.08	.0158	1304	.444	4.34	103.2
		61.74	735	36.39	.201	31.13	.0171	1384	.531	4.36	102.7
		62.13	736	36.22	.199	30.83	.0179	1384	.408	4.28	109.4
		62.29	735	36.13	.198	30.66	.0179	1374	.475	4.32	102.8
		61.79	735	36.32	.201	31.06	.0201	1443	.474	4.52	102.8
	II	62.36	735	40.09	0.220	33.94	0.0160	1307	0.414	5.12	103.0
		62.53	735	40.07	.219	33.86	.0179	1374	.402	5.18	103.8
		62.26	736	40.18	.221	39.11	.0201	1449	.456	5.31	104.0
		62.68	735	36.35	.198	30.63	.0159	1299	.449	4.34	102.4
		62.35	734	36.80	.201	31.16	.0157	1297	.414	4.50	103.2
		62.55	736	36.74	.200	31.05	.0178	1368	.436	4.37	103.3
		62.62	735	36.77	.200	31.01	.0207	1468	.412	4.36	104.0
		62.72	737	36.81	.201	31.08	.0179	1364	.467	4.58	102.0
Takeoff	I	63.27	855	37.10	0.218	36.06	0.0167	1421	0.294	6.12	101.0
		61.93	856	35.83	.215	35.59	.0185	1487	.277	5.89	102.6
		61.92	858	35.99	.216	35.84	.0201	1536	.257	5.94	102.3
		63.44	857	34.25	.200	33.24	.0188	1495	.237	4.99	102.3
		61.06	853	34.13	.207	34.27	.0177	1457	.234	5.35	102.3
	S-I	63.03	863	36.42	0.215	35.85	0.0150	1375	0.469	4.92	100.5
		62.51	859	36.75	.219	36.30	.0163	1415	.501	5.22	100.6
		63.27	861	36.69	.216	35.90	.0175	1454	.526	5.06	100.6
		61.97	860	33.92	.203	33.85	.0151	1374	.479	4.44	100.0
		62.50	860	33.75	.199	33.36	.0162	1407	.516	4.32	99.9
		62.09	860	33.94	.203	33.81	.0182	1469	.526	4.61	99.8
	II	62.35	861	36.92	0.221	36.64	0.0152	1383	0.316	5.32	101.3
		62.03	861	37.23	.229	37.10	.0179	1469	.313	5.43	101.7
		62.43	863	37.01	.221	36.74	.0221	1603	.354	5.31	102.1
		62.62	862	34.14	.205	34.15	.0142	1345	.333	4.73	101.3
		62.85	862	34.12	.202	33.75	.0171	1441	.303	4.47	101.3
		62.35	861	34.15	.202	33.67	.0184	1484	.323	4.53	101.3
	S-II	61.83	863	36.37	0.219	36.47	0.0162	1425	0.567	4.26	102.3
		62.32	861	36.11	.221	35.87	.0174	1463	.693	4.14	102.5
		61.84	859	36.52	.220	36.47	.0187	1501	.742	4.30	102.4
		62.13	828	38.54	.227	36.92	.0161	1387	.656	4.58	101.7
		62.24	828	38.52	.226	36.81	.0171	1423	.715	4.54	102.7

TABLE III. - COMBUSTOR EXHAUST EMISSION DATA

Design condition	Combustor model	Oxides of nitrogen, $NO_x = NO + NO_2$, ppm	Oxides of nitrogen, $\frac{g\ NO_2}{kg\ fuel}$	Unburned hydrocarbons, ppm	Unburned hydrocarbons, $\frac{g\ CH_2}{kg\ fuel}$	Carbon monoxide, ppm	Carbon monoxide, $\frac{g\ CO}{kg\ fuel}$	Carbon dioxide, ppm	Carbon dioxide, $\frac{g\ CO_2}{kg\ fuel}$	Ratio of gas sample to measured fuel-air ratio, $\frac{(f/a)_{gs}}{(f/a)_m}$	Combustor gas analysis efficiency, η_{gs}, percent
Cruise	I	87.9	8.7	6.3	0.20	148.4	8.9	33 695	3189	1.014	99.77
		113.2	9.7	2.5	.10	94.1	4.9	40 370	3306	1.049	99.88
		124.2	9.7	1.6	.03	87.3	4.2	44 180	3304	1.049	99.90
		130.0	10.0	1.4	.02	81.6	3.8	45 156	3309	1.050	99.91
		132.6	10.1	1.2	.02	84.0	3.9	45 289	3297	1.047	99.91
		130.1	9.2	1.6	.03	87.9	3.8	48 499	3266	1.037	99.91
		99.9	8.9	3.6	.09	103.3	5.6	37 025	3143	.997	99.90
		118.4	9.3	2.1	.05	80.2	3.8	41 771	3249	1.031	99.93
		151.1	10.3	1.4	.03	66.1	2.7	49 931	3266	1.037	99.91
	S-I	130.1	11.6	25.0	0.70	267	14.0	39 893	3132	0.916	99.59
		151.6	12.3	18.7	.50	229	11.0	36 773	3138	.911	99.69
		116.2	11.9	20.4	.63	211.6	13.2	31 556	3145	1.002	99.63
		126.1	12.0	16.4	.47	205.7	11.9	34 766	3163	1.008	99.67
		136.4	12.4	19.2	.52	202.4	11.2	36 206	3139	1.000	99.69
		138.1	12.5	18.7	.51	210.7	11.6	33 427	2895	.982	99.68
		156.5	12.7	16.5	.40	210.9	10.4	36 730	2853	.987	99.71
	II	74.6	7.5	22.3	0.68	256.9	15.8	32 721	3160	1.009	99.56
		88.7	8.04	15.5	.38	212.1	11.2	37 099	3093	.985	99.70
		103.6	8.37	10.8	.26	190.8	9.4	41 340	3193	1.016	99.75
		79.6	8.1	16.05	.49	208.4	12.9	32 522	3165	1.009	99.65
		77.9	8.0	16.8	.58	222.9	13.9	31 987	3145	1.003	99.62
		95.7	8.7	12.1	.33	174.7	9.7	34 302	3159	1.005	99.74
		116.0	9.1	8.4	.19	145.7	6.9	42 126	3158	1.003	99.81
		96.0	8.7	10.0	.27	181.6	10.0	36 305	3150	1.002	99.74
Takeoff	I	131.7	12.8	0.9	0.03	47.4	2.8	34 680	3217	1.020	99.93
		156.2	13.7	.7	.02	36.7	2.0	38 911	3272	1.037	99.95
		175.1	14.2	.6	.01	32.9	1.6	41 965	3256	1.032	99.96
		174.7	15.1	.5	.01	30.4	1.6	39 919	3296	1.045	99.96
		149.9	13.7	.5	.01	38.2	2.1	37 034	3252	1.031	99.95
	S-I	149.3	16.1	2.1	0.07	78.7	5.2	30 311	3133	0.994	99.87
		160.9	16.0	2.0	.06	76.2	4.6	32 682	3109	.986	99.88
		178.7	16.6	1.7	.05	69.3	3.9	34 731	3085	.978	99.90
		152.7	16.4	1.7	.06	70.4	4.6	30 457	3122	.990	99.88
		166.5	16.7	1.5	.04	64.0	3.9	32 380	3101	.986	99.90
		188.9	16.9	1.3	.03	62.3	3.4	35 759	3058	.969	99.92
	II	129.4	13.7	1.5	0.05	67.7	4.4	31 238	3175	1.007	99.89
		153.9	13.9	1.2	.03	51.6	2.8	36 772	3189	1.001	99.93
		203.7	15.0	1.0	.02	50.1	2.2	44 760	3155	.954	99.94
		126.2	14.4	2.2	.07	83.7	5.8	28 906	3153	1.001	99.86
		163.1	15.5	1.4	.04	48.1	2.8	34 943	3171	1.005	99.93
		174.4	15.4	1.2	.03	41.3	2.2	37 770	3184	1.009	99.94
	S-II	160.6	16.0	1.5	0.04	85.7	5.21	31 648	3022	0.959	99.87
		182.4	17.0	1.4	.04	80.5	4.75	34 025	3152	.962	99.89
		191.4	17.4	1.2	.03	83.4	4.62	36 235	3152	.955	99.89
		126.9	12.8	4.7	.14	139.1	8.2	31 005	2984	.950	99.79
		141.5	13.5	2.9	.08	129.2	7.2	33 178	3021	.959	99.82

TABLE IV. - EFFECT OF FLAME STABILIZER DESIGN ON SEVERAL COMBUSTOR PARAMETERS AT NOMINAL INLET CONDITIONS

[Inlet-air temperature, 855 K; inlet Mach number, 0.22, fuel-air ratio, 0.018.]

Model number	Pattern factor, $\bar{\delta}$	Pressure loss, $\Delta P/P$, percent	Oxides of nitrogen emission index, NO_x
I	0.28	5.89	13.7
II	.31	5.43	13.9
S-I	.53	5.06	16.6
S-II	.69	4.14	17.0

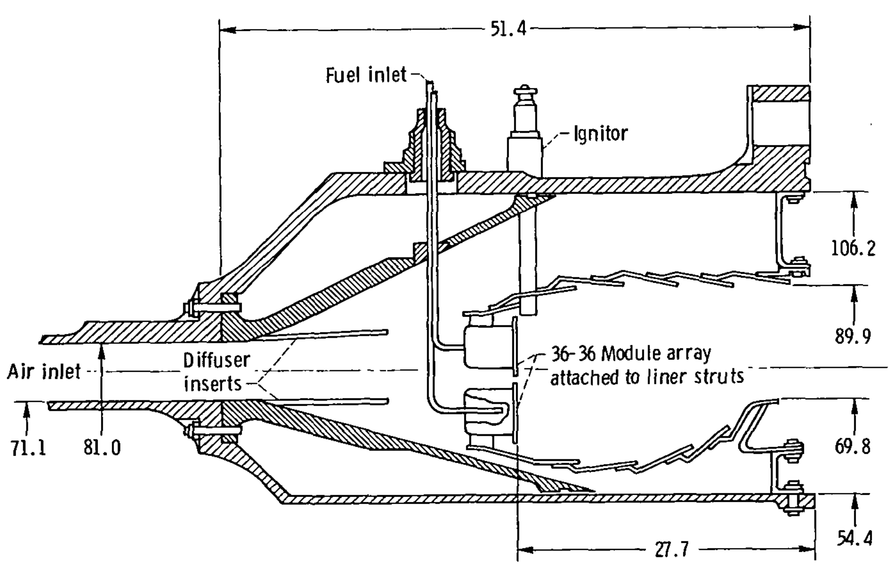

Figure 1. - 36-36 Module swirl-can combustor configuration. (Dimensions are in cm.)

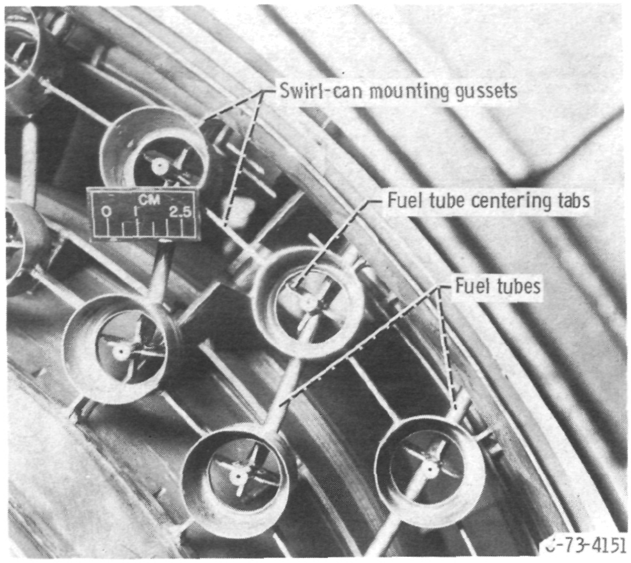

Figure 2. - 36-36 Module swirl-can mounting technique and fuel tube centering tabs.

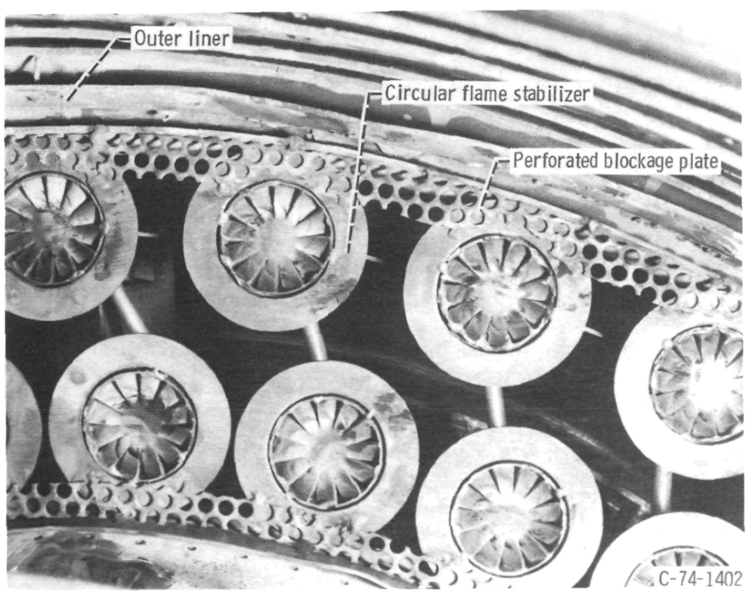

Figure 3. - Model I swirl-can combustor with circular flame stabilizer.

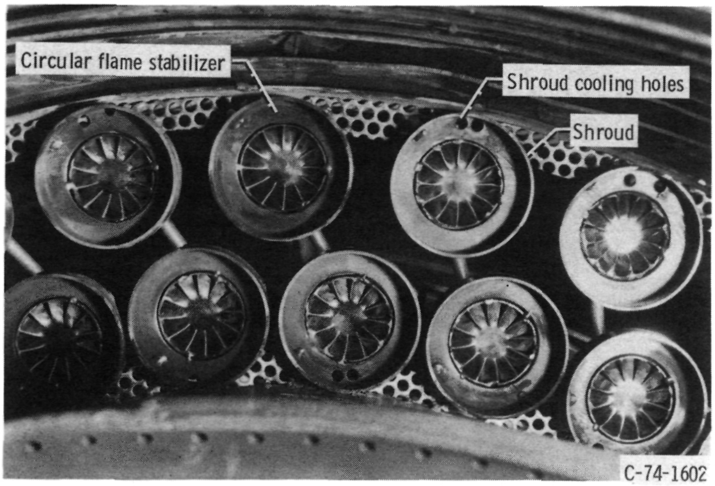

Figure 4. - Model S-I swirl-can combustor with circular flame stabilizer and shrouds.

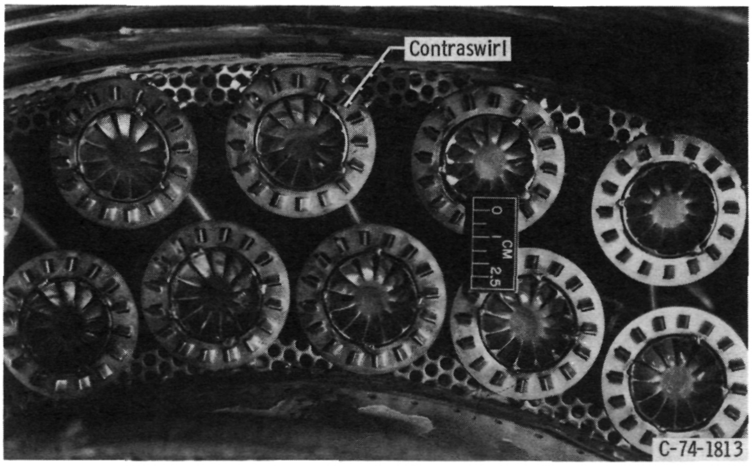

Figure 5. - Model II swirl-can combustor with contraswirl flame stabilizers.

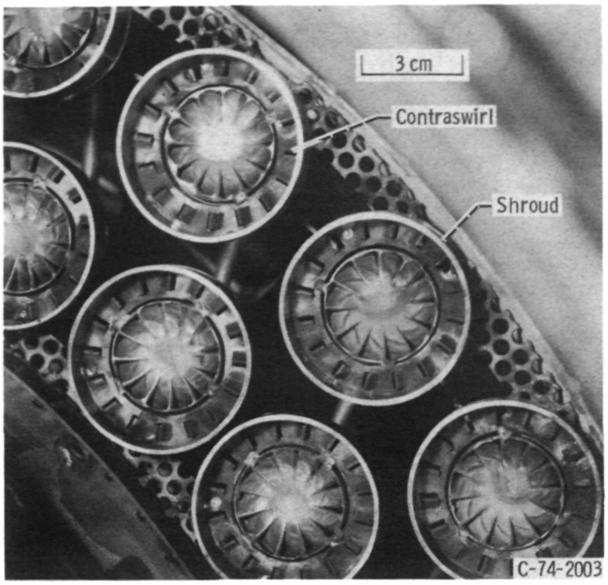

Figure 6. - Model S-II swirl-can combustor with contraswirl flame stabilizers and shrouds.

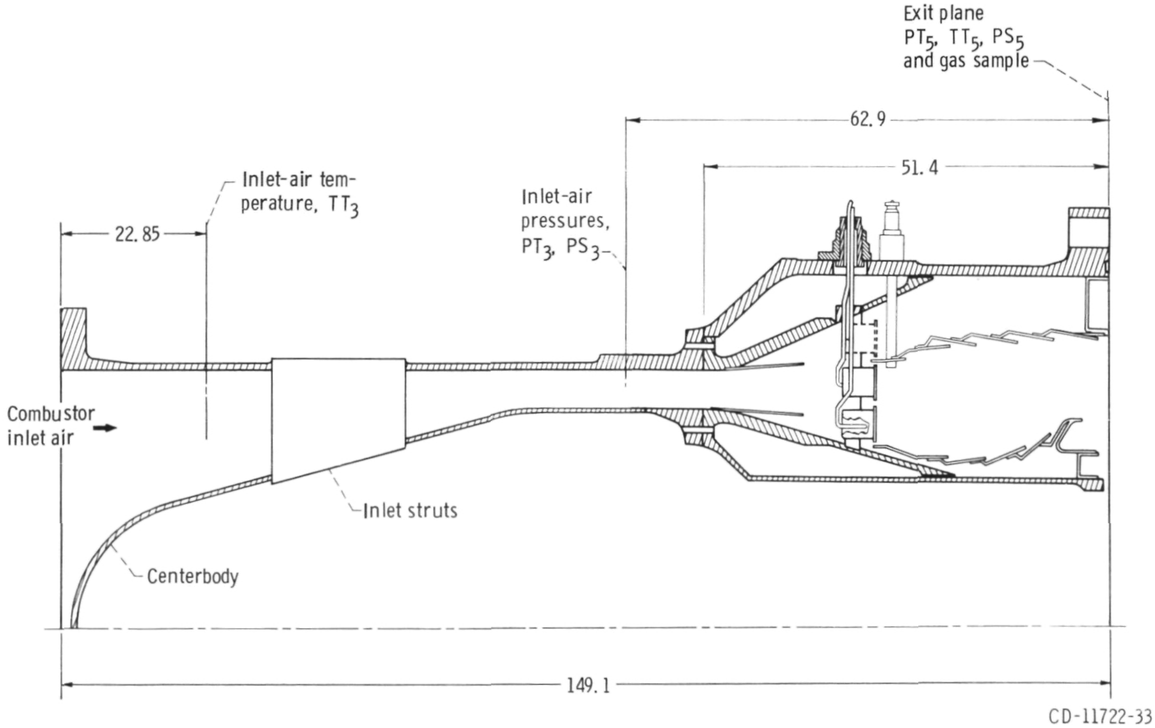

Figure 7. - Combustor housing and test section showing axial instrumentation planes. (Dimensions are in cm.)

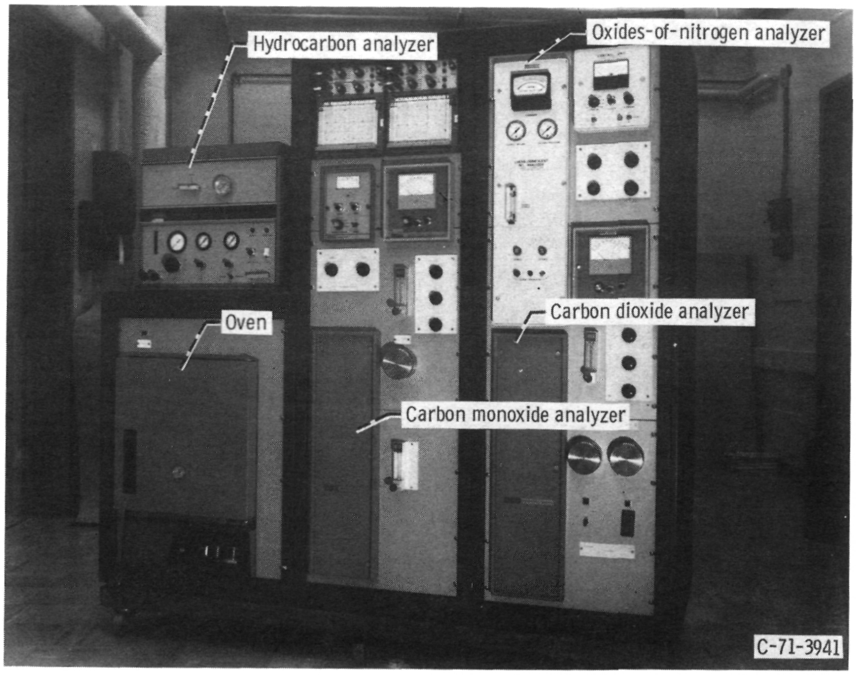

Figure 8. - Gas sampling instrument console.

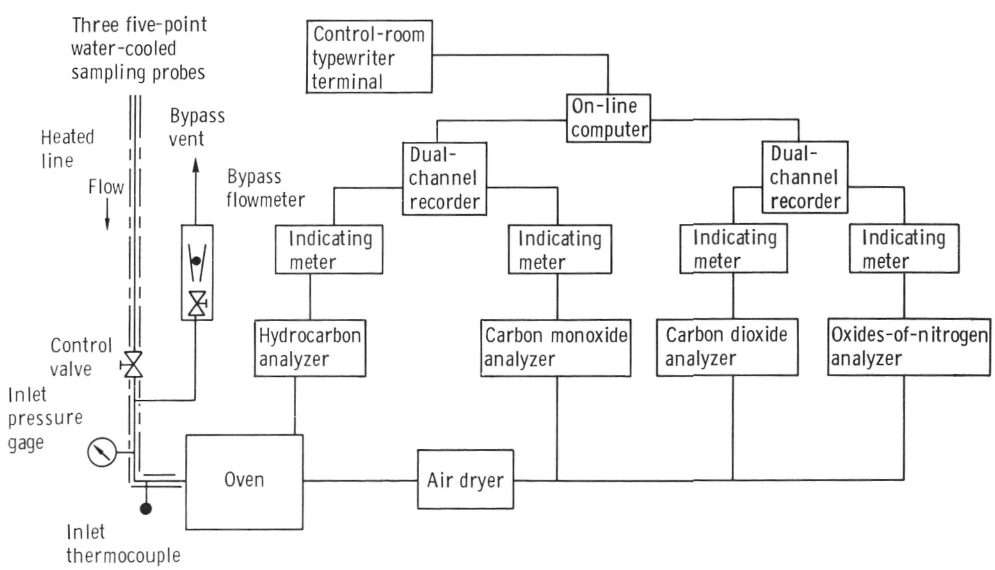

Figure 9. - Schematic diagram of gas analysis system.

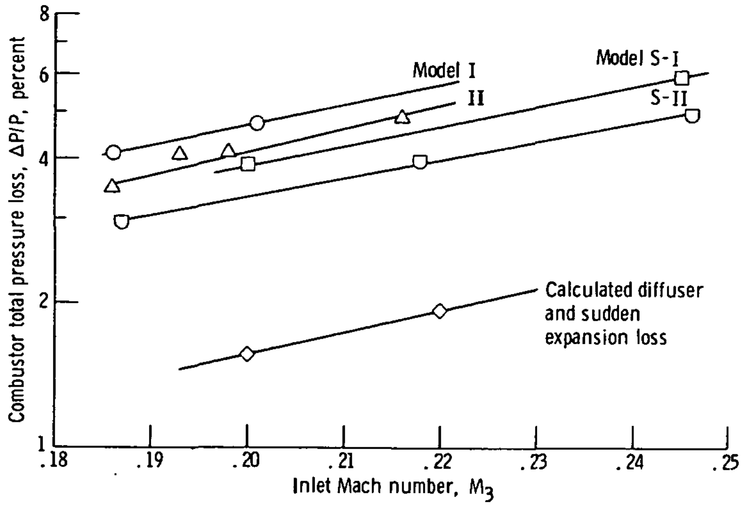

Figure 10. - Combustor isothermal pressure loss against inlet Mach number.

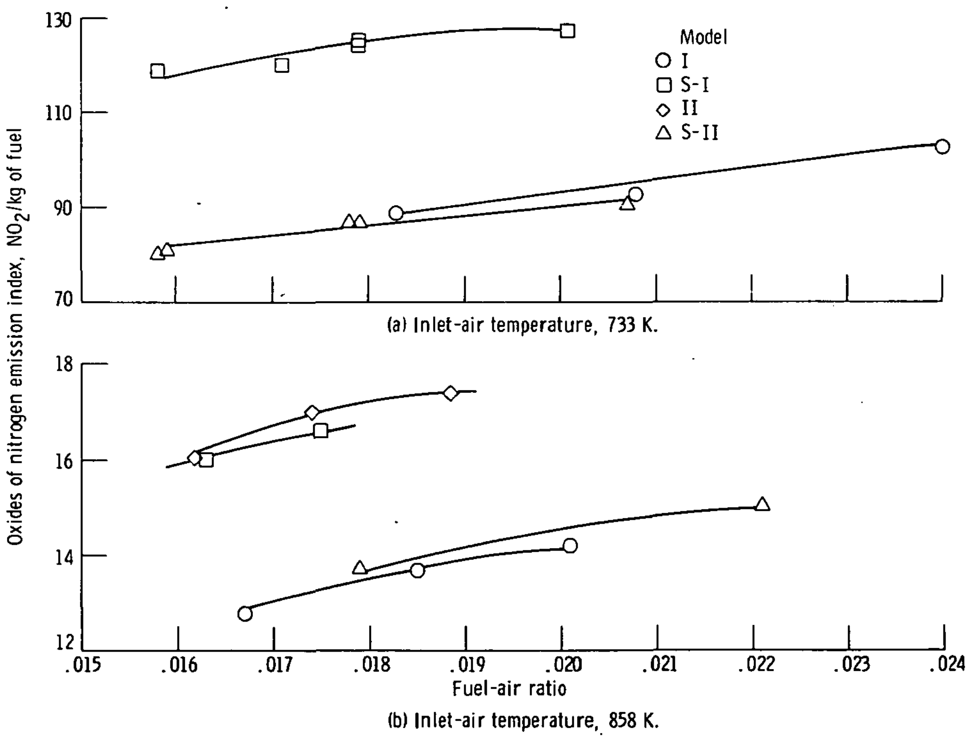

Figure 11. - Effect of combustor fuel-air ratio on oxides of nitrogen at simulated take-off conditions. Reference velocity, 36.6 meters per second; inlet total pressure, 62 newtons per square centimeter.

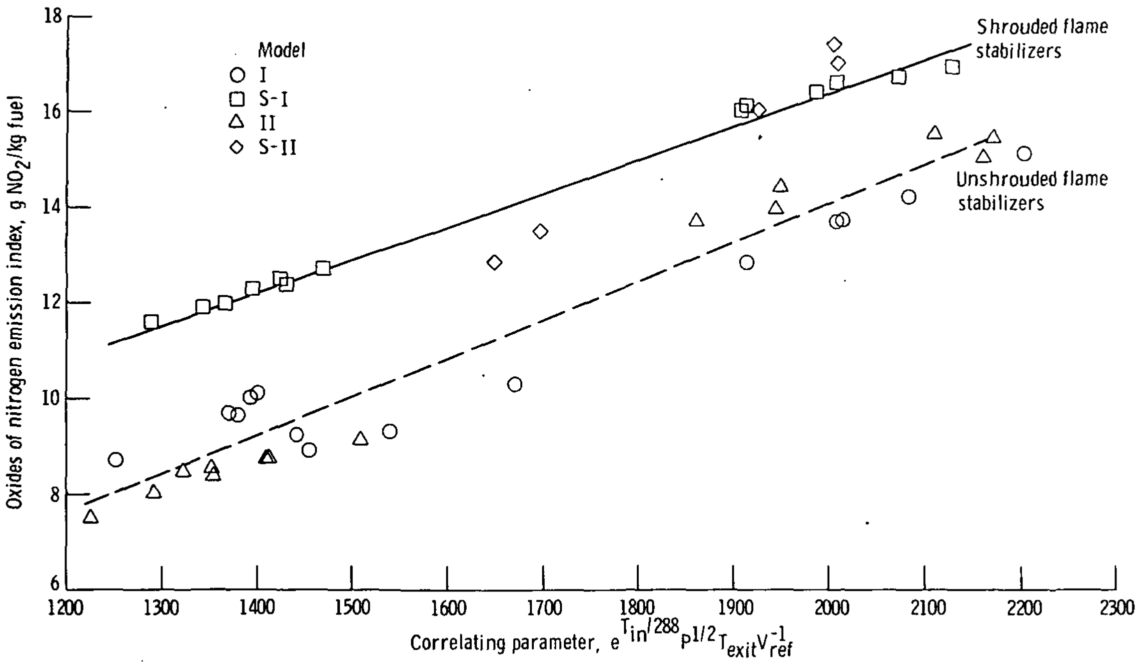

Figure 12. - Data fit curves of tested combustor designs showing oxides of nitrogen against correlating parameter.

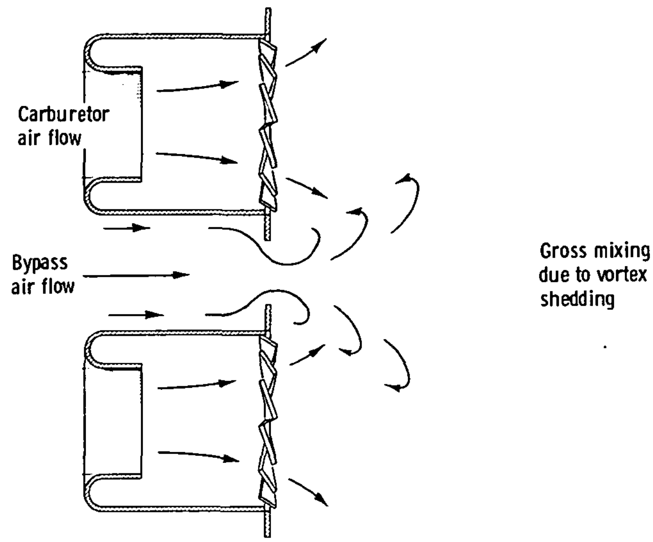

(a) Unshrouded.

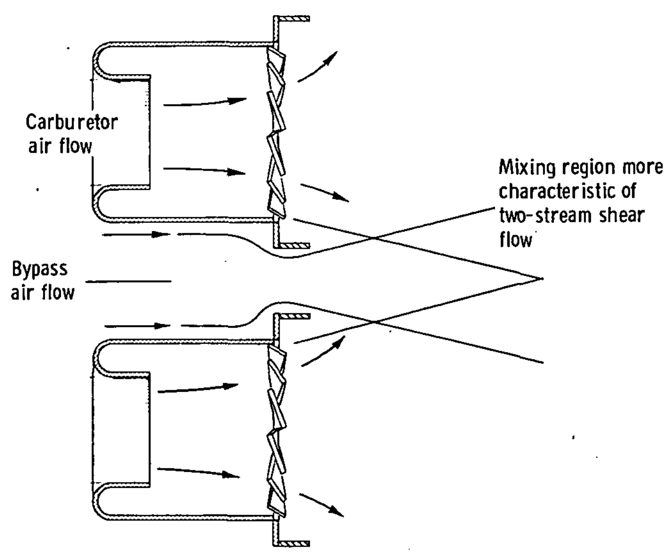

(b) Shrouded

Figure 13. - Mixing patter of shrouded and unshrouded flame stabilizers.

NATIONAL AERONAUTICS AND SPACE ADMINISTRATION
WASHINGTON, D.C. 20546

OFFICIAL BUSINESS
PENALTY FOR PRIVATE USE $300

SPECIAL FOURTH-CLASS RATE
BOOK

POSTAGE AND FEES PAID
NATIONAL AERONAUTICS AND
SPACE ADMINISTRATION
451

U.S.MAIL

POSTMASTER: If Undeliverable (Section 158 Postal Manual) Do Not Return

"The aeronautical and space activities of the United States shall be conducted so as to contribute . . . to the expansion of human knowledge of phenomena in the atmosphere and space. The Administration shall provide for the widest practicable and appropriate dissemination of information concerning its activities and the results thereof."

—NATIONAL AERONAUTICS AND SPACE ACT OF 1958

NASA SCIENTIFIC AND TECHNICAL PUBLICATIONS

TECHNICAL REPORTS: Scientific and technical information considered important, complete, and a lasting contribution to existing knowledge.

TECHNICAL NOTES: Information less broad in scope but nevertheless of importance as a contribution to existing knowledge.

TECHNICAL MEMORANDUMS: Information receiving limited distribution because of preliminary data, security classification, or other reasons. Also includes conference proceedings with either limited or unlimited distribution.

CONTRACTOR REPORTS: Scientific and technical information generated under a NASA contract or grant and considered an important contribution to existing knowledge.

TECHNICAL TRANSLATIONS: Information published in a foreign language considered to merit NASA distribution in English.

SPECIAL PUBLICATIONS: Information derived from or of value to NASA activities. Publications include final reports of major projects, monographs, data compilations, handbooks, sourcebooks, and special bibliographies.

TECHNOLOGY UTILIZATION PUBLICATIONS: Information on technology used by NASA that may be of particular interest in commercial and other non-aerospace applications. Publications include Tech Briefs, Technology Utilization Reports and Technology Surveys.

Details on the availability of these publications may be obtained from:

SCIENTIFIC AND TECHNICAL INFORMATION OFFICE

NATIONAL AERONAUTICS AND SPACE ADMINISTRATION

Washington, D.C. 20546